ALGORITH BASED ON MEDIUM CO-OCCURRENCE MATRIX FOR IMAGE REGION CLASSIFICATION

DAN POPESCU, RADU DOBRESCU, MAXIMILIAN NICOLAE, VALENTIN AVRAM
Department of Control and Computers
POLITEHNICA University of Bucharest
Splaiul Independentei nr. 313, Bucharest 6,
ROMANIA

Abstract: The paper presents a method for the classification and identification of texture image regions. To compare regions, a data base with single texture images is used. The dimension of the reference images is greater than the analyzed region dimension. For the proper region recognition a decision theoretic method and two types of statistic texture feature are used. The first type features are the peak of grey level histogram and the texton contour pixel densities (edge densities) per unit of area. The second type features derive from the medium co-occurrence matrices: contrast, energy, entropy, homogeneity, and variance. The algorithms are implemented in Visual C++2005 and Matlab and allows the simultaneously display of both the investigated regions pairs, and the euclidian distance between them. Our experimental results indicate the fact that the selected features which derive from medium co-occurrence matrices have a good discriminating power for texture classification. The results also confirm the fact that the distances between the similar regions are relatively small and the distances between regions from different textured images are relatively great.

Key-words: Texture, Statistic features, Medium co-occurrence matrix, Edge densities, Image difference, Grey level histogram, Image classification.

1 Introduction

It is very hard to define rigorously the texture into an image. The texture can be considered like a structure which is composed by many similar elements (patterns) named textons or texels, in some regular or continual relationship.

Texture analysis has been studied using various approaches, like statistical type (grey level co-occurrence matrices and the features extracted from them, autocorrelation based features, power spectrum, etc), and structural type. In the last case, the texture are composed of primitives, and an image description is produced by the placement of these primitives according to certain placement rules.

The structural approach is suitable for analyzing textures with more regularity in the placement of texture elements.

The statistical approach utilises features to characterize the stochastic properties of the distribution of grey levels in the image.

There are two important kinds of problems that texture analysis research attempts to solve: texture segmentation and texture classification. Another problem, texture synthesis is often used for image compression application.

The process called texture segmentation consists in identifying regions with similar texture and separating regions with different texture.

Texture classification involves deciding what texture class an observed image belongs to. Thus, one needs to have an a priori knowledge of the classes to be recognized. The major focus of this paper is the classification process based on medium co-occurrence matrix features.

An experimental study has been conducted to classify some regions of textured images. With this end in view, the whole image is partitioned in four equivalent regions like in Fig.1. Different textured regions are compared based on minimum distance between measured features which are derived from medium co-occurrence matrices (contrast, energy, entropy, homogeneity, and variance) or by contour pixel densities.

Our experimental results indicate that the five features selected from medium co-occurrence matrices have a good discriminating power in texture classification applications.

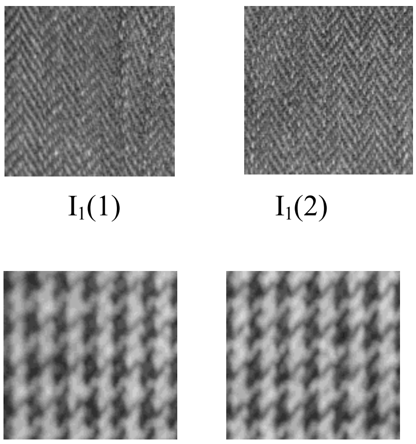

$I_1(1)$ $I_1(2)$

$I_2(1)$ $I_2(2)$

Fig. 1. Image regions derived from two images (I_1 and I_2) with different textures.

2 Statistical methods to texture analysis

The statistical approach is more useful than structural approach to texture analysis. The simplest statistical features like the mean (1) and standard deviation (3) can be computed indirectly in terms of the image histogram h.

Thus,

$$\mu = \frac{1}{N}\sum_{i=1}^{K} x_i h(x_i) \tag{1}$$

$$N = \sum_{i=1}^{K} h(x_i) \tag{2}$$

$$\sigma^2 = \frac{1}{N}\sum_{i=1}^{K}(x_i - \mu)^2 h(x_i) \tag{3}$$

where $N = n_1 n_2$ is the image dimension, and K is the number of grey levels.

The shape of an image histogram provides many clues to characterize the image, but sometimes it is inadequately to discriminate textures (it is not possible to indicate local intensity differences).

Another simple statistic features is the edge density per unit of area, Den_e (4). The density of edges, detected by a local binary edge detector, can be used to distinguish between fine and coarse texture like in Fig.1. Den_e can be evaluated by the ratio between the pixel number of extracted edges (which must be tinned – one pixel thickness) and image area (pixel number of region matrix):

$$Den_e = \frac{N_e}{A} \tag{4}$$

In ecquation (4), N_e represents the number of edge pixels (tinned edges, with one pixel thickness) and A is the region area.

In order to characterize textured images, connected pixels must be analysed. For this reason, correlation function (5), difference image (6) in certain direction $d = (\Delta x, \Delta y)$, and co-occurrence matrices (9), must be considered:

$$R(x,y) = \frac{\sum_{u=0}^{n_1-1}\sum_{v=0}^{n_2-1} I(u,v)\, I(u+x, v+y)}{\sum_{u=0}^{n_1-1}\sum_{v=0}^{n_2-1} I^2(u,v)} \tag{5}$$

$$I_d(x,y) = I(x,y) - I(x+\Delta x\ , y+\Delta y) \tag{6}$$

From histogram of difference image h_d, one can extract the mean (7) and standard deviation (8):

$$\mu_d = \frac{1}{N}\sum_{i=1}^{K} x_i h_d(x_i) \tag{7}$$

$$\sigma_d^2 = \frac{1}{N}\sum_{i=1}^{K}(\ x_i - \mu_d\ )^2 h_d(x_i) \tag{8}$$

The most powerful statistical method to textured image analysis is based on features extracted from the Grey-Level Co-occurrence Matrix (GLCM), proposed by Haralick in 1973 (Haralick 1973). GLCM is a second order statistical measure of image variation and it gives the joint probability of occurrence of grey levels of two pixels separated spatially by a fixed vector distance $d=(\Delta x, \Delta y)$. Smooth texture gives co-occurrence matrix with high values along diagonals for small d. The range of grey level values within a given image determines the dimensions of a co-occurrence matrix. Thus, 4 bits grey level images give 16x16 co-occurrence matrices. The elements of a co-occurrence matrix C_d depend upon displacement $d=(\Delta x, \Delta y)$:

$$C_d(i,j) = Card\{((x,y),(t,v))/I(x,y) = i,\ I(t,v) = j,\ (x,y),\ (t,v) \in N \times N,\ (t,v) = (x+\Delta x,\ y+\Delta y)\} \quad (9)$$

From a co-occurrence matrix C_d one can draw out some important statistical features for texture classification. These features, which have a good discriminating power, were proposed by Haralick (Haralick 1973, Haralick 1992): contrast (10), entropy (10), energy (11), homogeneity (12). The contrast measures the coarseness of texture. Large values of contrast correspond to large local variation of the grey level. The entropy measures the degree of disorder or non-homogeneity. Large values of entropy correspond to uniform GLCM. The energy is a measure of homogeneity.

3 Local features derived from medium co-occurrence matrix

For each pixel we consider increasing (2d+1)x(2d+1) symmetric neighborhoods, d = 1, 2, 3,...,10. Inside each neighborhood there are 8 principal directions: 1, 2, 3, 4, 5, 6, 7, 8 (Fig. 2) and we evaluated the co-ocurence matrices $C_{d,k}$ corresponding to vector distances determined by the central point and the neighborhood edge point in the k direction (k=1,2,...,8). For each neighborhood type, an average co-ocurence matrix C_d is calculated (10):

$$C_d = 1/8(C_{d,1} + C_{d,2} + C_{d,3} + C_{d,4} + C_{d,5} + C_{d,6} + C_{d,7} + C_{d,8}),\ d = 1,2,\ldots,10 \quad (10)$$

Thus, for 3x3 neighborhood, d = 1; for 5x5 neighborhood, d = 2; for 7x7 neighborhood, d = 3; for 9x9 neighborhood, d = 4, and so on.

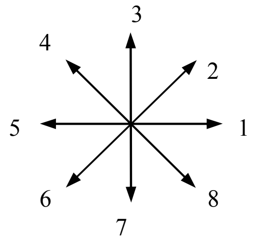

Fig. 2. Principal direction for co-ocurence matrix calculus.

In order to quantify the spatial dependence of gray level values, from average co-ocurence matrices C_d, d = 1, 2,..., 10, we calculate various textural features like Contrast – Con_d – (11), Energy – Ene_d – (12), Entropy – Ent_d – (13), Homogeneity – Omo_d – (14) and Variance – Var_d – (15).

$$Con_d = \sum_{i=1}^{L}\sum_{j=1}^{L}(i-j)^2 C_d(i,j) \quad (11)$$

$$Ene_d = \sum_{i=1}^{L}\sum_{j=1}^{L} C_d(i,j)^2 \quad (12)$$

$$Ent_d = -\sum_{i=1}^{L}\sum_{j=1}^{L} C_d(i,j)\log(C_d(i,j)) \quad (13)$$

$$Omo_d = \sum_{i=1}^{L}\sum_{j=1}^{L}\frac{C_d(i,j)}{1+|i-j|} \quad (14)$$

$$Var_d = \frac{1}{L}\sum_{i=1}^{L}\sum_{j=1}^{L}[C_d(i,j) - \overline{C_d(i,j)}]^2 \quad (15)$$

4 Experimental results and discusion

For alghoritm testing and program validation we used two textured images I_1 and I_2, each partitioned in four regions $I_i(1)$, $I_i(2)$, $I_i(3)$, $I_i(4)$, i=1,2 (Fig. 3).

$I_1(1)$	$I_1(2)$
$I_1(3)$	$I_1(4)$

Fig. 3. Four regions image partition.

In fact, the regions are 128 x 128 images whith 16 grey levels.
From these images we considered two regions for I_1 image, and two regions for I_2 image, $I_i(1)$, $I_i(2)$ – Fig. 3.

Firstly, the analysis of the simple grey level histogram (Fig. 4, Fig. 5, Fig. 6, Fig. 7) demonstrates that the regions can be discriminated by the aid of the mode location and mode value (histogram peak) which is greater for $I_1(1)$ and $I_1(2)$ than for $I_2(1)$ and $I_2(2)$. Seccondly, supposing that the histograms are not so different, another set of texture features makes possible the region classification. Thus, we can consider the co-occurence matrices and the features derived from them. Because the first and the last lines and columns are full with 0, one can elimine them. So the co-occurence matrix dimension becomes 14 x 14 (Fig.8).

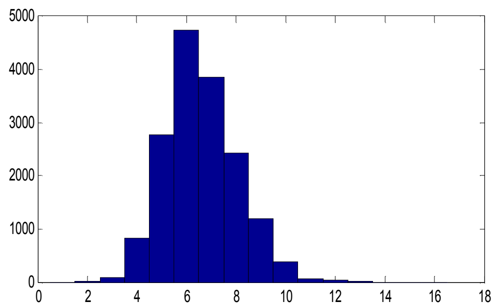

Fig. 4. Grey level histogram for $I_1(1)$.

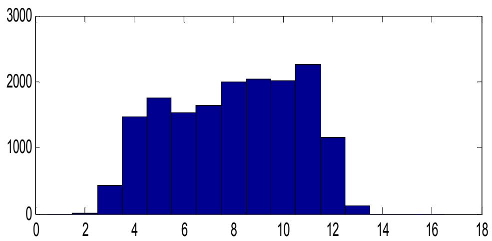

Fig. 5. Grey level histogram for $I_1(2)$.

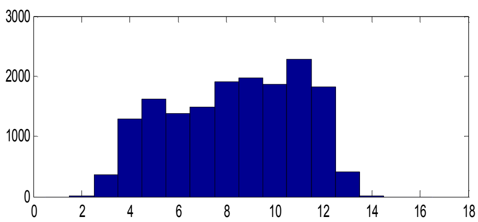

Fig. 6. Grey level histogram for $I_2(1)$.

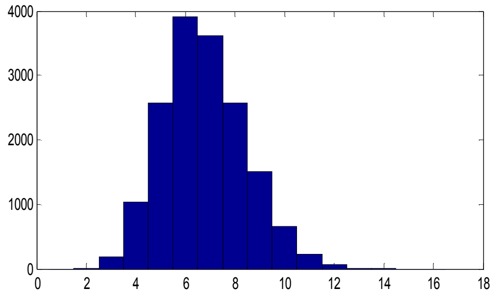

Fig. 7. Grey level histogram for $I_2(2)$.

Table 1. Five statistical texture derived from co-occurence matrices.

d	Image	Con_d	Ene_d	Ent_d	Omo_d	Var_d
1	$I_1(1)$	0.39	1.17	1.01	0.93	0.34
1	$I_1(2)$	0.60	0.81	0.96	0.84	0.46
1	$I_2(1)$	0.13	0.98	1.00	1.16	1.04
1	$I_2(2)$	0.15	0.89	0.99	1.13	1.17
2	$I_1(1)$	0.63	1.01	0.98	0.81	0.33
2	$I_1(2)$	0.88	0.73	0.93	0.75	0.45
2	$I_2(1)$	0.38	0.57	0.90	0.92	1.02
2	$I_2(2)$	0.45	0.52	0.89	0.88	1.15
3	$I_1(1)$	0.65	0.99	0.97	0.79	0.33
3	$I_1(2)$	0.89	0.72	0.92	0.73	0.45
3	$I_2(1)$	0.72	0.42	0.85	0.78	1.00
3	$I_2(2)$	0.85	0.38	0.84	0.75	1.14
4	$I_1(1)$	0.64	0.97	0.96	0.79	0.32
4	$I_1(2)$	0.87	0.70	0.91	0.73	0.44
4	$I_2(1)$	1.07	0.34	0.81	0.69	0.99
4	$I_2(2)$	1.25	0.32	0.81	0.66	1.13
5	$I_1(1)$	0.70	0.94	0.94	0.75	0.32
5	$I_1(2)$	0.95	0.68	0.89	0.70	0.44
5	$I_2(1)$	1.41	0.30	0.79	0.62	0.98
5	$I_2(2)$	1.62	0.28	0.79	0.60	1.12
6	$I_1(1)$	0.67	0.91	0.93	0.75	0.32
6	$I_1(2)$	0.90	0.67	0.88	0.70	0.43
6	$I_2(1)$	1.70	0.28	0.77	0.57	0.97
6	$I_2(2)$	1.94	0.26	0.77	0.56	1.11
7	$I_1(1)$	0.60	0.90	0.92	0.76	0.31
7	$I_1(2)$	0.78	0.66	0.87	0.72	0.42
7	$I_2(1)$	1.95	0.27	0.76	0.53	0.96
7	$I_2(2)$	2.21	0.25	0.76	0.52	1.10
8	$I_1(1)$	0.58	0.89	0.90	0.76	0.31
8	$I_1(2)$	0.78	0.64	0.86	0.71	0.42
8	$I_2(1)$	2.16	0.27	0.75	0.50	0.95
8	$I_2(2)$	2.43	0.25	0.75	0.49	1.08
9	$I_1(1)$	0.58	0.88	0.89	0.75	0.30
9	$I_1(2)$	0.78	0.63	0.84	0.70	0.41
9	$I_2(1)$	2.31	0.27	0.74	0.48	0.95
9	$I_2(2)$	2.60	0.25	0.74	0.47	1.07
10	$I_1(1)$	0.54	0.85	0.88	0.76	0.30
10	$I_1(2)$	0.75	0.62	0.83	0.70	0.41
10	$I_2(1)$	2.41	0.27	0.73	0.46	0.93
10	$I_2(2)$	2.72	0.25	0.73	0.46	1.06

Textural features like Con_d – (8), Ene_d – (9), Ent_d – (10), Omo_d – (11), and Var_d – (12) are calculated. The normalised results are presented in Table 1, for d = 1,2,...,10.

$$
\begin{matrix}
0 & 0 & 0 & 0 & 0 & 0 & 0 & 0 & 0 & 0 & 0 & 0 & 0 & 0 \\
0 & 1 & 2 & 0 & 0 & 0 & 0 & 0 & 0 & 0 & 0 & 0 & 0 & 0 \\
0 & 2 & 255 & 139 & 13 & 1 & 0 & 0 & 0 & 0 & 0 & 0 & 0 & 0 \\
0 & 0 & 139 & 845 & 372 & 67 & 4 & 0 & 0 & 0 & 0 & 0 & 0 & 0 \\
0 & 0 & 13 & 372 & 831 & 376 & 122 & 11 & 0 & 0 & 0 & 0 & 0 & 0 \\
0 & 0 & 1 & 67 & 376 & 533 & 402 & 125 & 11 & 0 & 0 & 0 & 0 & 0 \\
0 & 0 & 0 & 4 & 122 & 402 & 519 & 446 & 125 & 5 & 0 & 0 & 0 & 0 \\
0 & 0 & 0 & 0 & 11 & 125 & 446 & 784 & 506 & 99 & 2 & 0 & 0 & 0 \\
0 & 0 & 0 & 0 & 0 & 11 & 125 & 506 & 832 & 499 & 52 & 0 & 0 & 0 \\
0 & 0 & 0 & 0 & 0 & 0 & 5 & 99 & 499 & 896 & 489 & 11 & 0 & 0 \\
0 & 0 & 0 & 0 & 0 & 0 & 0 & 2 & 52 & 489 & 1383 & 308 & 1 & 0 \\
0 & 0 & 0 & 0 & 0 & 0 & 0 & 0 & 0 & 11 & 308 & 767 & 53 & 0 \\
0 & 0 & 0 & 0 & 0 & 0 & 0 & 0 & 0 & 0 & 1 & 53 & 66 & 0 \\
0 & 0 & 0 & 0 & 0 & 0 & 0 & 0 & 0 & 0 & 0 & 0 & 0 & 0
\end{matrix}
$$

Fig. 8. Co-occurence matrix C_1 for $I_2(1)$ image.

For the purpose of discriminated power evaluation of the selected features we calculated the euclidian distances between regions from the same image: $D\{I_1(1),I_1(2)\}$, $D\{I_2(1),I_2(2)\}$, and the euclidian distances between regions from different images: $D\{I_1(1),I_2(1)\}$, $D\{I_1(1),I_2(2)\}$, $D\{I_1(2),I_2(1)\}$, $D\{I_1(2),I_2(2)\}$. The euclidian distance $D\{I_1, I_2\}$ between two images I_1 and I_2, which are characterized by the feature vectors $[C_1,E_1,Et_1,O_1,V_1]^T$ and $[C_2,E_2,Et_2,O_2,V_2]^T$ is expressed by the following relation:

$$D(I_1,I_2)=\sqrt{(C_1-C_2)^2+(E_1-E_2)^2+(Et_1-Et_2)^2+(O_1-O_2)^2+(V_1-V_2)^2}$$

where: $C = Con$, $E = Ene$, $Et = Ent$, $O = Omo$, $V = Var$. In the Table 2, the results of mentioned distances calculus are presented.

From Table 2, one can observe that the distances between two different regions, like $D\{I_1,I_2\}$, are greater than distances between two similar regions, like $D\{I_1,I_1\}$ or $D\{I_2,I_2\}$. In order to apreciate the efficiency of the presented algorithm, we analyzed the most unfavourable cases, namelly the minimum distance between two regions coming from different images, and the maximum distance between two regions coming from the same image. These distances are grouped in two categories , for d = 1,2,…,5 and d = 6,7,…,10 (Table 3). Thus, $D_{min}\{I_1,I_2\}$ is grater than $\max\{D_{Max}\{I_1,I_1\}, D_{Max}\{I_2,I_2\}\}$, especially in large neighbourhood case (d=6,7,…,10).

Table 2. Euclidian distances between different images

d	D $\{I_11,I_12\}$	D $\{I_31,I_32\}$	D $\{I_11,I_31\}$	D $\{I_11,I_32\}$	D $\{I_12,I_31\}$	D $\{I_12,I_32\}$
1	0,44	0,16	0,81	0,93	0,83	0,89
2	0,40	0,16	0,87	0,98	0,79	0,86
3	0,39	0,19	0,89	1,04	0,66	0,67
4	0.38	0,22	1,03	1,22	0,70	0,88
5	0,39	0,25	1.18	1,40	0,81	1,04
6	0,36	0,27	1,40	1,65	1,06	1,31
7	0,33	0,29	1,65	1,92	1,36	1,64
8	0,34	0,30	1,83	2,12	1,54	1,83
9	0,34	0,31	1,97	2,27	1,68	1,99
10	0,34	0,34	2,09	2,42	1,79	2,13

Table 3. Minimum and maximum distances.

d=1,2,…,5

Images	D_{min}	D_{Max}
$D\{I_1,I_1\}$	0,38	0,40
$D\{I_2,I_2\}$	0,16	0,25
$D\{I_1,I_2\}$	0,66	1,40

d=6,7,…,10

Images	D_{min}	D_{Max}
$D\{I_1,I_1\}$	0,33	0,36
$D\{I_2,I_2\}$	0,27	0,34
$D\{I_1,I_2\}$	1,06	2,42

Concluding remarks

Because it is considered a medium omnidirectional co-occurrence matrix, the presented algorithm is relatively insensible to image translation and rotation. The results confirm that the statistic second order features, extracted from these co-occurrence matrices, especially in the case d = 6,7,…,10, offer a good discriminating power in texture identification process. The main application of the algorithm consists in texture identification and classification of the regions in multitextured images (like images from satellite or images from video camera of intelligent vehicles).

Towards ameliorate the classification accuracy, a development of the recognition algorithm, consisting in the attachment of new textural features like edge point density per unit of area and statistical features extracted from histogram of difference image, is proposed. Thus, we considered an edge extraction algorithm, based on imge binarisation and logical function [11], which gives tinned edges. The edge densities for the analized regions $I_1(1)$, $I_1(2)$, $I_2(1)$, and $I_2(2)$ show that this feature has also a good discriminating power (Table 4) and the combination with the previously second order type statistical features will give better results in texture classification.

Table 4. Edge densities of the analyzed regions.

Region	N_e	*A*	Den_e
I_1 (1)	5818	16384	0.3551
I_1 (2)	5820	16384	0.3552
I_2 (1)	3481	16384	0.2125
I_2 (2)	3296	16384	0.2012

References

[1] Haralick, R.M. et al. - Textural Features for Image Classification, IEEE Trans. on Systems, Man. And Cybernetics, vol.SMC-3, no.6, nov.1973, pp 610-621;

[2] Haralick, R.M., Shapiro, L.G. - Computer and Robot Vision, Add.-Wesley, Pub. Co., 1992;

[3] Tamura, H.; Mori, S.; Yamawaki, T. - Texture features corresponding to visual perception, IEEE Trans. On Systems, Man and Cybernetics. 6(4):460-473, 1976;

[4] Niblack, W. et al. - The QBIC Project: Querying Images by Content Using Color, Texture and Shape, Proc. of the Conference Storage and Retrieval for Image and Video Databases, SPIE vol.1908, pp.173-187, 1993;

[5] Liu, F. and Picard, R.W. - Periodicity, directionality and randomness: World features for image modeling and retrieval, IEEE Transactions on Pattern Analysis and Machine Intelligence 18(7):722-733, 1996;

[6] Manjunath, B.S. and Ma, W.Y. - Texture features for browsing and retrieval of large image data, IEEE Transactions on Pattern Analysis and Machine Intelligence,(Special Issue on Digital Libraries), Vol. 18 (8), August1996, pp. 837-842;

[7] Kaplan, L.M. et al. - Fast texture database retrieval using extended fractal features, in Storage and Retrieval for Image and Video Databases VI (Sethi, I K and Jain, R C, eds.), Proc SPIE 3312, 162-173, 1998;

[8] Smith, J. - Integrated Spatial and Feature Image System: Retrieval, Analysis and Compression, Ph. D. Thesis, Columbia University, 1997;

[9] Deng,Y. - A Region Representation for Image and Video Retrieval, Ph. D. thesis, University of California, Santa Barbara, 1999;

[10] Ma, W.Y. - Netra: A Toolbox for Navigating Large Image Databases, Ph. D. thesis, University of California, Santa Barbara, 1997.

[11] Popescu, D., Dobrescu, R., Avram, V., Mocanu, St. – Dedicated Primary Image Processors For Mobile Robots, WSEAS Trans. on Systems, Issue 8, Vol.5, August 2006, p. 1932-1939